

Dipolar coupling and multidomain states in perpendicularly polarized nanostructures

Alexei N. Bogdanov* and Ulrich K. Rößler†
IFW Dresden,
P.O. Box 270116, D-01171 Dresden, Germany
 (Dated: November 13, 2021)

Stripe states in multilayer systems with perpendicular polarization are investigated by analytical calculations within a general continuum approach, applicable to ferromagnetic, ferroelectric, or ferroelastic nanoscale superlattices. The competition between the long-range depolarization effect and short-range interlayer couplings can stabilize monodomain states and unusual stripe phase ground states with antiparallel polarization in adjacent layers. Geometric parameters of stable stripe domain states and the phase transitions lines between single domain states, aligned and antialigned stripe states have been derived. The theory is applied to analyze multidomain states and phase transitions in antiferromagnetically coupled multilayers [CoPt]/Ru.

PACS numbers: 75.70.Cn, 75.70.Kw, 77.80.-e, 77.80.Dj,

Multidomain states considerably influence physical properties of condensed matter systems with spontaneous polarization. Such spatially inhomogeneous patterns form ground states of ferromagnetic [1, 2], ferroelectric [3], or ferroelastic [5] films. Recently multidomain structures have been observed in nanoscale magnetic films and multilayers with strong perpendicular anisotropy [12, 13, 14, 16, 17] and in ferroelectric superlattices [3, 4, 11]. Similar spatially modulated states can also arise in polar or magnetic liquid crystals [19, 20], polar multiblock copolymer layers [21], in superconducting films or magnetic-superconductor hybrids [22], and in shape memory alloy films [23]. Multilayer systems with perpendicular polarization components provide ideal experimental models to investigate fundamental aspects of ordered structures and stable pattern formation in confining geometries. Control of such regular depolarization patterns is also of practical interest. E.g., patterns may provide templates, which could be decorated by nanoparticles or macromolecules, or they may be used to calibrate imaging techniques. Particular interest in ferroelectric superlattices is driven by the exciting possibility of using ferroelectric nanostructures in nonvolatile memory applications, new microelectromechanical systems (MEMS), and for nonlinear optics devices [3]. In nanomagnetism, antiferromagnetically coupled superlattices with strong perpendicular anisotropy [13, 14, 16] are considered as promising candidates for nonvolatile magnetic recording media and other applications [6]. According to recent experiments [3, 13, 14] these nanoscale superlattices are characterized by new multidomain states, unusual depolarization processes, and other specific effects which have no counterpart in other classes of media with perpendicular polarization.

We present here a detailed analysis of multidomain states in magnetic nanoscale superlattices with perpendicular polarization components. We derive simplified micromagnetic equations for equilibrium parameters of stripe domains in nanoscale multilayer systems. These mathematical tools provide a clear description of the multidomain processes and reveal the physical mechanism underlying their unconventional properties. It was found that in contrast to other bulk and nanomagnetic systems, the magnetic states here are determined by a close competition between interlayer exchange and dipolar couplings. The enhanced stray field couplings are responsible for the unusual switching processes and specific transformation of the domain patterns observed in synthetic metamagnetic multilayer systems, as [CoPt]/Ru and others [13, 14, 16]. The depolarization effects revealed in this paper have a universal character. They arise similarly in ferroelectric superlattices and in other nanosized polarized media.

For definiteness we consider stripe domains in magnetic nanolayers. We analyse superlattices consisting of N identical layers with thickness h separated by spacer layers of thickness s (Fig. 1). The perpendicular anisotropy fixes the easy magnetization direction. Within the single layers the magnetization $\mathbf{M}_i(\mathbf{r})$, may be spatially inhomogeneous. The energy can be written in a phenomenological approach as

$$W_N = \sum_{i=1}^{N-1} \int \int j(\mathbf{r}_i, \mathbf{r}_j) \mathbf{M}_i \cdot \mathbf{M}_{i+1} dv_i dv_j + \quad (1)$$

$$\sum_{i=1}^N \int \left[-\frac{K}{2} (\mathbf{M}_i \cdot \mathbf{n})^2 - \mathbf{H}^{(e)} \cdot \mathbf{M}_i - \frac{1}{2} \mathbf{H}_d \cdot \mathbf{M}_i \right] dv_i$$

where integrals are over the volume v_i of the single layers. $\mathbf{H}^{(e)}$ and $\mathbf{H}_d(\mathbf{r})$ are the externally applied and the depolarizing magnetic fields, respectively. The unity vector \mathbf{n} designates the normal to the film. $K > 0$ is a perpendicular anisotropy. The short-range interlayer coupling parameter between (nearly) homogeneous layers $J = \int \int j(\mathbf{r}_i, \mathbf{r}_j) dv_i dv_j > (<) 0$ favours (anti)parallel

*Permanent address: Donetsk Institute for Physics and Technology, 340114 Donetsk, Ukraine ; Electronic address: a.bogdanov@ifw-dresden.de

†Corresponding author ; Electronic address: u.roessler@ifw-dresden.de

orientation of the neighbouring layers. To investigate general effects of competing stray field and exchange interlayer interactions, we consider a simple model of a multidomain structure, namely stripe domains with antiparallel magnetization of magnitude $M \equiv |\mathbf{M}_i| = \text{const}$ within all the magnetic layers. The adjacent domains are separated by *thin* domain walls with energy density σ . The magnetic field \mathbf{H} is applied perpendicular to the layer surfaces. The stripe structure is described by the widths of domains d_{\pm} that are polarized in the directions parallel (+) and antiparallel (-) to the field. The geometry of stripes in a multilayer structure is conveniently defined by the stripe period $D = d_+ + d_-$, and a set of reduced parameters

$$q = \frac{d_+ - d_-}{D}, \quad p = 2\pi \frac{h}{D}, \quad \nu = \frac{s}{h}, \quad \tau = 1 + \nu, \quad (2)$$

where q is proportional to the average magnetization in a stripe structure, p is the reduced thickness of single ferromagnetic layers, ν is the thickness ratio between magnetized layer and interlayer, and τ fixes the superlattice period (Fig. 1).

The reduced energy $w_N = W_N/(2\pi M^2 N)$ of a system with N can be written

$$w_N = \frac{2\Lambda p}{\pi^2} - \frac{Hq}{2\pi M} + \varkappa \left(1 - \frac{1}{N}\right) + w_m(p, q). \quad (3)$$

In Eq. (3), the term linear in p is the energy of the domain walls. The next two terms are Zeeman energy and the short-range interlayer coupling, respectively. The stray field energy $w_m(p, q)$ must be derived by solving the corresponding magnetostatic problem [9]. The reduced energy (3) depends on the two dimensionless materials parameters

$$\varkappa = \frac{J}{2\pi M^2}, \quad \Lambda = \pi \frac{l}{h}. \quad (4)$$

The strengths of the exchange coupling is measured by \varkappa given by the ratio between the exchange and stray field energies. The parameter Λ characterizes the balance between the domain wall energy and stray field energies. It is fixed by the ratio of *characteristic length*, $l = \sigma/(4\pi M^2)$, which is a fundamental material parameter, see Ref. 2) and the thickness of the magnetic layers.

Due to the mathematical identity of electro- and magnetostatic equations [2] the multilayer with stripes can be thought of as a set of planes with “charged” stripes (Fig. 1). For two such planes separated by an interlayer with thickness $a = \omega h$, the magnetostatic energy is

$$f(\omega) = \frac{4}{p} \sum_{n=1}^{\infty} \frac{1 - (-1)^n \cos(nq)}{n^3} \exp(-np\omega). \quad (5)$$

The stray-field energy of the “charges” within the same plane is $w_m^{(0)} = q^2 + f(0)$. The dipolar coupling energy between the “poles” on different sides of the same layer

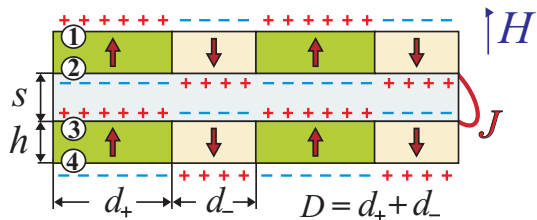


FIG. 1: A fragment of a superlattice: two ferromagnetic nanolayers (of thickness h) with stripe domains are separated by a nonmagnetic spacer of thickness s . The domains are coupled by the exchange (J) and magnetostatic forces.

is $f(1)$. Hence, the magnetostatic energy of individual layers is [7, 8]

$$w_m^{(\text{self})} = q^2 + f(0) - f(1) \quad (6)$$

The stray field energy of the multilayer, w_m originally derived by Suna,[9] can be written as a sum of “self” energies of the layers and interactions between them

$$\begin{aligned} w_m &= w_m^{(\text{self})} + w_m^{(\text{int})}, \\ w_m^{(\text{int})} &= \pm \frac{1}{N} \sum_{k=1}^{N-1} (N-k) F_k, \\ F_k &= f(\tau k + 1) + f(\tau k - 1) - 2f(\tau k). \end{aligned} \quad (7)$$

The upper (lower) signs in $w_m^{(\text{int})}$ correspond to parallel (antiparallel) arrangement of the polarization in adjacent layers (Figs. 2, 3). We denote these modes as *ferro* (F) or *antiferro* (AF) stripes. The factors F_k equals stray field coupling energies between two layers separated by distance τk . They are composed of the four contributions of the magnetodipole coupling between pairs of the planes bounding the layers. In particular, for two adjacent layers, $k = 1$ (Fig. 1), the interactions $1 \leftrightarrow 3$ and $2 \leftrightarrow 4$ yield equal (positive) energy contributions $f(\tau)$, while $1 \leftrightarrow 4$ and $2 \leftrightarrow 3$ yield negative energy contributions, $f(\tau + 1)$ and $f(\tau - 1)$, correspondingly.

In common polarized systems with characteristic sizes far beyond the nanoscale range the equilibrium domain sizes are usually much smaller than the individual layer thicknesses, $p \gg 1$. Numerous observations indicate that, as soon as domain sizes approaches the layer thickness, coercivity suppresses the formation of regular multidomain patterns [2]). This establishes a natural limit for domain sizes in classical systems. For $D \ll h$ there is no effective dipole interaction between different surfaces. Hence, in Eq.(7) for all nonzero ω , one has $f(\omega) \ll f(0)$, and the stray field energy of the multilayer is reduced to $w_m^{(0)}$ [1]. In such decoupled superlattices the multidomain states should have similar properties as those in isolated layers.

On the contrary, in perpendicular polarized nanoscale films and multilayers the periods of *regular* multidomain patterns is of the same order as their thicknesses or exceed these thicknesses [4, 12, 14]. In such systems dipole

interactions between different surfaces have a sizable effect. Mathematically, this is seen from slowly converging sums of interaction terms between poles far apart and on different internal surfaces. For such structures, numerical evaluation becomes arduous, and sharpened analytical methods are required. To overcome the slow convergence in w_m , we extend the method introduced in [27]. With the help of the identity $\int_0^\infty t^{(m-1)} \exp(-nt) dt = m!/n^m$, the infinite sums in Eq. (5) can be transformed into integrals on the interval $[0, 1]$

$$f(\omega) - f(0) = \pi^2(1 - q^2) - 2p\Omega(\omega) \quad (8)$$

where

$$\Omega(\omega) = \omega^2 \int_0^1 (1-t) \ln \left[1 + \frac{\cos^2(\pi q/2)}{\sinh^2(\omega pt/2)} \right] dt. \quad (9)$$

Then the dipolar stray field energy (7) can be written as

$$w_m = 1 - \frac{2p}{\pi^2} \Omega(1) \pm \frac{2p}{\pi^2 N} \sum_{k=1}^{N-1} (N-k) \Xi_k(\tau k), \quad (10)$$

$$\Xi_k(\tau k) = 2\Omega(\tau k) - \Omega(\tau k + 1) - \Omega(\tau k - 1). \quad (11)$$

Minimization of w_N (3) with respect to p and q yields the equilibrium parameters of the stripes in the multilayers. By the form of the multilayer energy Eq. (3) the widths of the stripes are independent of the interlayer couplings \varkappa . A complete analysis of these equations in applied field will be published elsewhere [28]. Here we investigate the ground state of the system in zero applied field, $\mathbf{H} = 0$. In this case $q = 0$ and the parameter p is derived from the equation $dw_N/dp = 0$

$$\Lambda = \Omega_p(1) \mp \frac{1}{N} \sum_{k=1}^{N-1} (N-k) \Xi_k^{(p)}(\tau k + 1) \quad (12)$$

where $\Xi_k^{(p)}(\tau k + 1) = 2\Omega_p(\tau k) - \Omega_p(\tau k + 1) - \Omega_p(\tau k - 1)$, and $\Omega_p(\omega) = d\Omega/dp(\omega)$. After elementary transformations this function can be written

$$\Omega_p(\omega) = -2\omega^2 \int_0^1 t \ln \left[\tanh \left(\frac{pt}{2} \right) \right] dt. \quad (13)$$

Typical solutions of Eq. (12) are presented in Figs. 2 and 3.

Ferro stripes. These solutions exist for any layer thickness Fig. 2. In the limit of thick layers the period D increases, while it tends to infinity as h tends to zero. The role of the stray-field couplings changes with the ratio of the interlayer thickness to the thickness of the polarized layers, ν . For the limiting cases of small and large thickness of the spacer layer given by the limits $\nu \ll 1$ or $\nu \gg 1$, respectively, the dependence $D(h)$

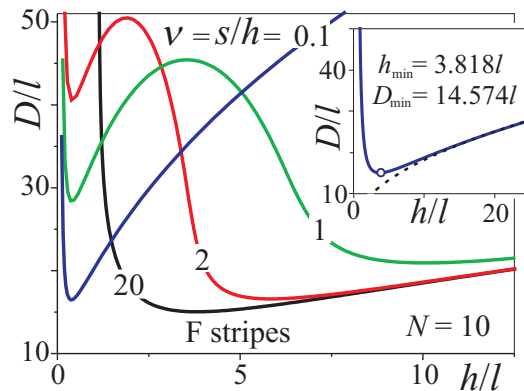


FIG. 2: The equilibrium reduced period D/l as a function of the reduced layer thickness h/l for ferro (F) stripes in an $N = 10$ multilayer for different values of parameter ν . Inset shows the function $D/l(h/l)$ for an isolated layer [7] and the parameters of the minimum point. Dashed line indicates $D \propto \sqrt{h}$ fit corresponding to Kittel theory.

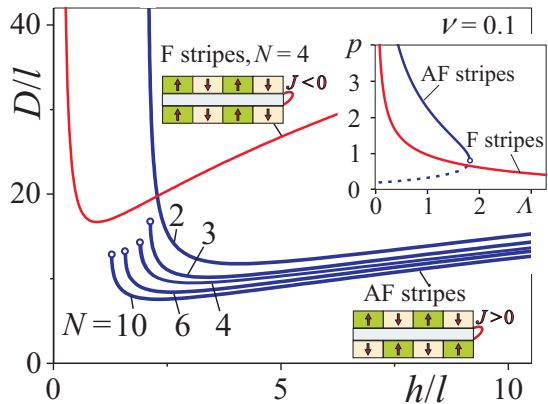


FIG. 3: The solutions $D/l(h/l)$ for ferro and antiferro (AF) stripes in systems with $\nu = 0.1$. AF stripes exist for thickness larger than the critical thickness h_{cr} . For a two-layer systems ($N = 2$) the stripe period goes to infinity at the critical thickness. For systems with $N > 2$ the critical stripe period D_{cr} has finite values. The thin (red) line shows the dependence $D(h)/l$ for the period of F stripes in the case $N = 4$. The corresponding solutions $p(\Lambda)$ of Eq. (12) for these parameters are plotted in the Inset: F stripes (red) and AF (blue) lines. Dashed line indicates unstable solutions.

approaches a behaviour of isolated layers with thickness hN and h correspondingly. In the limit of small ratios ν the stripe period $D(h)$ approaches the period for a F stripe state in a single layer with an effective total polarized layer thickness hN . For very large separation between the polarized layers, i.e., for large ratios ν the stripe period is determined by the properties of the decoupled single layers with thickness h . The limiting solution for an isolated layer $D(h)$ (Inset Fig. 2) obtained by [7] (see also Ref. 2) has a minimum point with parameters ($h_{min}/l = 0.96067$, $D_{min}/l = 16.3136$). The nonmonotonic behaviour of $D(h)$ reflects the antagonistic role of magnetic charges in the formation of the equi-

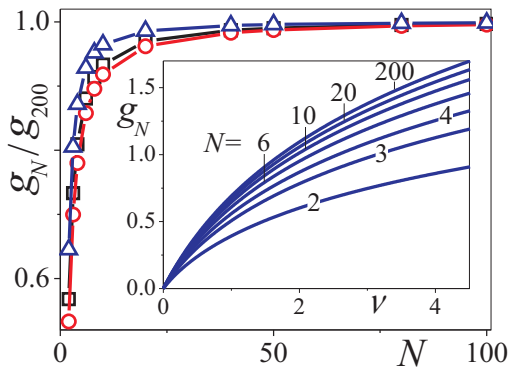


FIG. 4: The reduced values of the factor g_N as a function of N and different values of ν : 1 (\triangle), 5 (\square), 0.1 (\circ). Inset gives functions $g_N(\nu)$ for different values N .

librium stripes. In the case of small domains $D \ll h$, which is typical for classical systems, the dipole interaction between different surfaces of the layer is negligibly small, and only the interaction between charges on the same surface give a contribution to the stray field energy. For stripes with sizes $D \geq h$ the interaction between charges from different surfaces becomes a noticeable effect and counteracts the interactions between charges on the same surface. This can be understood as a screening effect. As the layer thickness decreases this screening effect becomes stronger and suppresses the stray field energy. As a result, for $h < h_{min}$ the extension of domains decreases both the sum of domain wall energies and the stray field energy, and the domain period increases exponentially with decreasing layer thickness. These simple energetical arguments demonstrate that in nanoscale multilayers, where domain sizes usually considerably exceed the thicknesses of magnetic and interlayer, h and s , the interaction between magnetic poles through the stack strongly influences the equilibrium magnetic states. Due to this effect a non-monotonous dependence of stripe periods $D(h)$ arises in multilayers between the limiting cases of large/small values both of ν and h , as shown in 2.

AF stripes. In this case the solutions of Eq. (12) $p(\Lambda)$ exist on the finite interval $\Lambda < \Lambda_{cr}$ and consist of two branches with stable and unstable solutions (Fig. 3, Inset). Correspondingly the equilibrium stripe states exist only in a finite range of the thickness $h < h_{cr}$ (Fig. 3). At a critical thickness h_{cr} the period reaches a critical value D_{cr} for multilayer systems with $N > 2$ and tends to infinity for two-layer system, $N = 2$, (Fig. 3).

In multilayers with a ferromagnetic coupling ($J < 0$) both the stray fields and exchange interactions favour parallel arrangement of the magnetization across the stack. Hence, the F-stripe mode is the ground state in such multilayers. On the contrary, in systems with antiferromagnetic interlayer couplings, $J > 0$, the dipole and

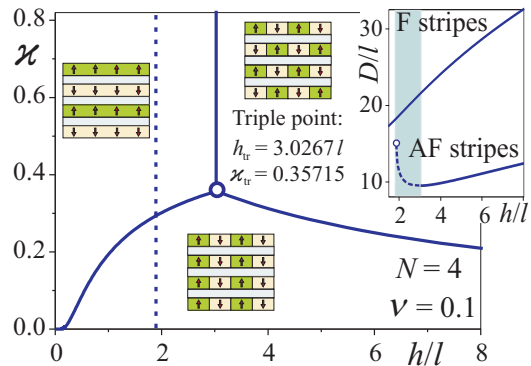


FIG. 5: The phase diagram of magnetic states in variables h/l and the reduced coupling \varkappa favouring antiparallel orientation of adjacent layers for $N = 4$. Thick lines indicate the first-order transitions between different phases. They meet in a triple point. The dashed line shows the stability limit of the AF stripes. Inset shows a difference between stripe periods in F and AF modes. Between the triple point and the critical point AF domains are metastable.

exchange forces have competing character. As a result, three different equilibrium phases can exist in such multilayers in zero field, see phase diagram Fig. 5. For sufficiently strong interlayer couplings a monodomain phase with antiparallel correlations of adjacent layers across the stack, and an AF stripe phase exist. The transition between the monodomain and AF stripe states for the two-layer system, $N = 2$, is continuous, as seen from the divergence of $D(h)$ (Fig. 3). For systems with $N \geq 3$ the transition is first-order. For weaker interlayer coupling \varkappa , the F stripe phase becomes stable. The transition between the F stripes and the AF stripes or monodomain state is a topological transition, and it is always first-order. At a triple point, that weakly depends on the multilayer repetitions N , all three phases coexist. Lines of first order transitions between the AF monodomain and AF stripe phase in dependence on N and layer thickness h are shown in Fig. 6.

In the limit of large domains ($D \geq l$) the expansion of the integral (9) for $q = 0$ yields $\Omega(\omega) = 3/2 - \ln(p\omega/2)$ and energy (3) can be transformed in the form

$$w_N = 1 - \frac{2p_N}{\pi^2} \left[\frac{3}{2} - \ln\left(\frac{p_N}{2}\right) - \tilde{\Lambda}_N \right] + \varkappa \left(1 - \frac{1}{N} \right) \quad (14)$$

where $p_N = pN = 2\pi(hN)/D$, $\tilde{\Lambda}_N = \Lambda/N + g_N(\nu)$. Then, the energy w_N (14) has the form of the energy for an *isolated* layer (see [27]) with “effective” thickness hN . This means that in a system with large domains ($D \gg h$) the multilayer stack behaves as an effectively coupled single layer and the domain period approaches the solution for a single layer with a total polarized thickness hN with an effective characteristic parameter $\tilde{\Lambda}$.

The function $g_N(\nu)$ describes the influence of finite spacers on the magnetic properties of the multilayer via

the redistribution of the internal “charges” within the stack. This function is given by

$$g_N = -\frac{1}{N^2} \sum_{k=1}^{N-1} (N-k) \tilde{G}(\nu) - \ln N, \quad (15)$$

where $\tilde{G}(\nu) = 2\tilde{g}(\tau k) - \tilde{g}(\tau k + 1) - \tilde{g}(\tau k - 1)$ and $\tilde{g}(\omega) = \omega^2 \ln(\omega)$. The dependence of $g_N(\nu)$ on the number of layers N and the ratio $\nu = s/h$ is shown in Fig. 15. In the limit of small ν this function behaves as $g_N = a_N \nu$ where the factor

$$a_N = 2(1 - 1/N) \ln N - 4N^{-2} \sum_{k=1}^{N-1} k \ln k \quad (16)$$

varies from $\ln(2)$ for $N = 2$ to unity as N tends to infinity. The equilibrium domain period in the limit of large N is (cf. [27])

$$D = \pi h N \exp(\tilde{\Lambda}_N - 1/2). \quad (17)$$

Recently, stripe domains have been investigated in Co/Pt multilayers [13, 14, 15]. AF stripes have been observed in Co/Pt multilayers [13]. F stripes have been investigated in a set of multilayers $[\text{Co}(4\text{\AA}) \text{Pt}(7\text{\AA})]_X$ (with X from 5 to 160) [15]. The average domain width $D/2$ in our notation plotted versus the total multilayer thickness is close to the line typical for an isolated layer (Inset, Fig. 2), the minimum point (h_{min}, D_{min}) is in the region $X \approx 20$ with a period D about 150 nm. This system has $\nu_f = 7/4 = 1.75$. However, the existing data are insufficient for detailed analysis and comparison with a theoretical dependencies for $D(h)$ in the Fig. 2. More substantial results have been obtained on the investigation of antiferromagnetically coupled (via Ru) ferromagnetic blocks $[[\text{Co}(4\text{\AA}) \text{Pt}(7\text{\AA})]_{X-1} \text{Co}(4\text{\AA}) \text{Ru}(9\text{\AA})]_N$ (with $N = 2$ to 10 and $X = 2$ to 12), Ref. [14]. Strictly speaking magnetic properties of such ferromagnetic multilayers may strongly differ from those of single layers (see Fig. 2). However, according to the results of [15] these blocks can be modelled by a single effectively ferromagnetic layer with total thickness $h = 11X - 7\text{\AA}$. Hence, $\nu(X) = 9/(11X - 7)$ varies from 0.072 ($X = 12$) to 0.6 ($X = 2$). The stripe periods, $D = 260$ nm for $X = 8$ [15], are much larger than the layer thicknesses h ranging from 1.5 to 12.5 nm. Thus, the approach Eq. (14) can be applied to describe these multidomain states. In particular, the critical line $h_t(N)$ of the first order transition between the homogeneous antiferromagnetic state and F stripes is derived from the following equation

$$\pi^2 \varkappa (1 - 1/N)/2 = \exp(-\pi l/(hN) - g_N \nu + 1/2) \quad (18)$$

and plotted in the Inset of Fig. 6. It should be stressed that despite the fact that energy (14) has been reduced to the same functional form as the energy for an isolated layer, these two model have different physical properties. Namely the function $g_N(\nu)$ in Eq. (14) describes the influence of the internal “charges” on the equilibrium states

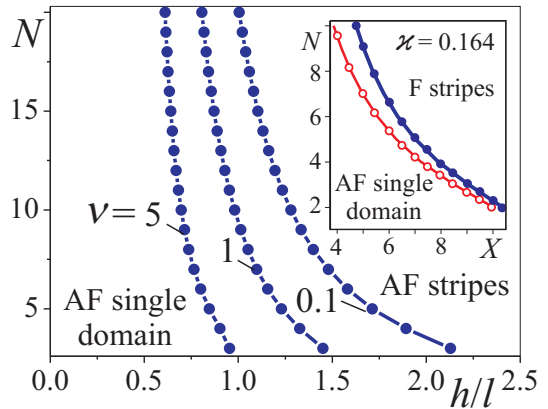


FIG. 6: The phase diagram in variables h/l and N with the critical lines between the antiferro single domain and the multidomain states. The transitional line between F stripes and AF single domain state (Inset, solid points) is in a close agreement with results obtained for magnetic Co/Pt multilayers in [14]. The line with hollow points indicates the transition in a model with zero internal charges ($g_N = 0$).

of stripes. The transition line $h_{t0}(N)$ between the antiferromagnetic homogeneous state and F stripes for an isolated layer ($g_N(\nu) = 0$) is plotted for comparison in the Inset of Fig. 6. The difference between the two line $(h_{t0} - h_t)/h_{t0} = sN/(\pi l)$ depends on the ratio s/l and increases with increasing N .

In conclusion, we have investigated a continuum approach for the stripe multidomains that arise as regular equilibrium depolarization structure of coupled multilayers. The zero-field phase diagram displays transitions between stripe states where adjacent layers are parallel due to depolarization effects and other phases where the layers are antiparallel under influence of short-range couplings. In this AF case, it is possible to stabilize monodomain states in thin multilayer systems. Furthermore, antiferro stripe phases can become stable in systems with sufficiently strong interlayer coupling. The transitions between these phases are first-order. In fact, within this model, the ferro stripe structure is metastable in the whole parameter range of the model. Therefore, the different multidomain phases can coexist in multilayer systems and are transformed into each other by domain nucleation and growth processes. Hence, severe hysteresis effects can arise in such multilayer systems subject to specific coercivity mechanisms. In particular the AF monodomain state can arise in the form of two domains that transform into each other by a global reversal of the magnetization structure. These domains can coexist out of equilibrium as remnant of an antiferro stripe state.

Acknowledgments. We thank I. Dragunov, O. Hellwig, N. Kiselev, J. McCord, V. Neu, and R. Schäfer for discussions. A.N.B. thanks H. Eschrig for support and hospitality at the IFW Dresden. This work was supported

-
- [1] C. Kittel, Phys. Rev. **70**, 965 (1946).
- [2] A. Hubert, R. Schäfer R., *Magnetic Domains* (Springer-Verlag, Berlin, 1998); V. G. Bar'yakhtar, et al. Usp. Fiz. Nauk. **156**, 47 (1988), [Sov. Phys. Usp. **31**, 810 (1988)].
- [3] M. Dawber, K. M. Rabe, J. F. Scott, Rev. Mod. Phys. **77**, 1083 (2005), J. F. Scott, Nanoferroelectrics: statics and dynamics J. Phys.:Cond. Mat. **18**, R361 (2006).
- [4] S.K. Streiffer, J. A. Eastman, D. D. Fong, C.Thompson, A. Munkholm, M.V. Ramana Murty, O. Auciello, G. R. Bai, G. B. Stephenson, Phys. Rev. Lett. **89**, 067601 (2002); D. D. Fong, G. B. Stephenson, S. K. Streiffer, J. A. Eastman, O.Auciello, P. H. Fuoss, C. Thompson, Science **304**, 1650 (2005); A. Schilling, T. B. Adams, R. M. Bowman, J. M. Gregg, G. Catalan, J. F. Scott, Phys. Rev. B **47**, 024115 (2006).
- [5] A. M. Bratkovsky, A. P. Levanyuk, Phys. Rev. Lett. **86**, 3642 (2001); Phys. Rev. B **65**, 094102 (2002).
- [6] E. E. Fullerton et al., IEEE Trans. Magn. **39**, 639 (2003); J. Åkerman, Science **308**, 508 (2005).
- [7] Z. Málek, V. Kamberský, Czech. J. Phys. **8**, 416 (1958).
- [8] C.Kooy, U. Enz, Philips Res. Repts. **15**, 7 (1960).
- [9] A. Suna, J. Appl. Phys. **59**, 313 (1985); H. J. G. Draaisma, W. J. M. de Jonge, J. Appl. Phys. **62**, 3318 (1987).
- [10] P. Grünberg, R. Schreiber, Y. Pang, M. B. Brodsky, and H. Sowers, Phys. Rev. Lett. **57**, 2442 (1986).
- [11] H.N. Lee, H.M. Christen, M.F. Chisholm, C.M. Rouleau, and D.H. Lowndes, Nature **433**, 395 (2005); J. Sigman, D. P. Norton, H. M. Christen, P.H. Fleming, L.A. Boatner, Phys. Rev. Lett. **88**, 097601 (2002); H. M. Christen, E. D. Specht, S. S. Silliman, K. S. Harshavardhan, Phys. Rev. B **68**, 020101R (2003).
- [12] V. Gehanno, Y. Samson, A. Marty, B. Gilles, A. Chamberod, J. Magn. Magn. Mater. **172**, 26 (1997).
- [13] S. Hamada, K. Himi, T. Okuno, K. Takanashi, J. Magn. Magn. Mater. **240**, 539 (2002).
- [14] O. Hellwig, et al. Nature Mater. **2**, 112 (2003); O. Hellwig, A. Berger, E. E. Fullerton, Phys. Rev. Lett. **91**, 197203 (2003);
- [15] J. Magn. Magn. Mater. **290-291**, 1 (2005).
- [16] H. Itoh, et al. J. Magn. Magn. Mater. **257** 184 (2003); Z.Y. Liu, S. Adenwalla, Phys. Rev. Lett. **91**, 037207 (2003).
- [17] U. K. Röbller, A. N. Bogdanov, Phys. Rev. B. **69**, 094405 (2004); J. Magn. Magn. Mater. **269**, L287 (2004); Phys. Rev. B. **69**, 184420 (2004).
- [18] A. M. Bratkovsky, A. P. Levanyuk, Phys. Rev. Lett. **84**, 3177 (2000); Phys. Rev. B **63**, 132103 (2001); V. A. Stephanovich, et al. Phys. Rev. Lett. **94**, 047601 (2005).
- [19] S. T. Lagerwall. Ferroelectric and Antiferroelectric Liquid Crystals (Wiley-VHC, Weinheim, 1999), L.U.Ruibou, et al. Jpn. J. Appl. Phys. **42**, 1628 (2003).
- [20] M. Sayar, M. Olivera de la Cruz, S.I. Stupp, Europhys. Lett. **61**, 334 (2003).
- [21] A.-V. Ruzette, L. Leibler, Nature Mater. **4** 19 (2005).
- [22] W. Gillijns, A. Y. Aladyshkin, M. Lange, M. J. Van Bael, V.V. Moshchalkov, Phys. Rev. Lett. **95**, 227003 (2005); V. Jeudy, C. Gourdon, and T. Okada, Phys. Rev. Lett. **92**, 147001 (2004).
- [23] J. W. Dong, J. Q. Xie, J. Lu, C. Adelman, C. J. Palmström, J. Cui, Q. Pan, T. W. Shield, R. D. James, J. Appl. Phys. **95**, 2593 (2004); A. N. Bogdanov, A. DeSimone, S. Müller, U.K. Röbller, J. Magn. Magn. Mater. **261**, 204 (2003).
- [24] S.-B. Choe, S.-C. Shin, Phys. Rev. B **59**, 142 (1999).
- [25] S.-B. Choe, S.-C. Shin, Phys. Rev. B **59**, 142 (1999).
- [26] M. Labrune, A. Thiaville, Eur. Phys. J. B **23**, 17 (2001).
- [27] A. N. Bogdanov, D. A. Yablonskii. Fiz. Tverd. Tela **22**, 680 (1980), [Sov. Phys. Solid State **22**, 399 (1980)].
- [28] N.S. Kiselev, I.E. Dragunov, U. K. Röbller, A. N. Bogdanov, to be published.
- [29] The particular behaviour of $D(h)$ was first obtained for a two-layer system in Ref. [28].